ChemComm

Accepted Manuscript

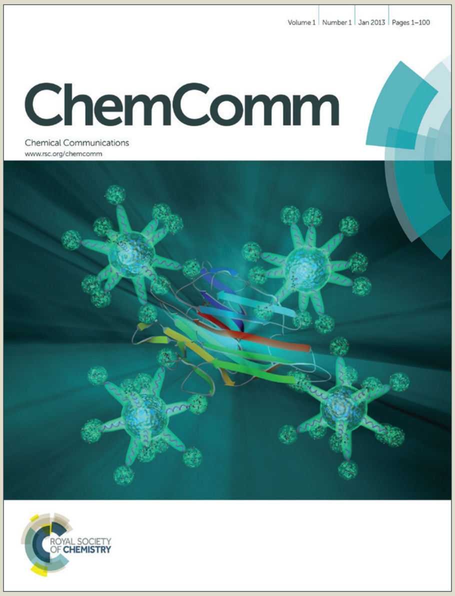

ROYAL SOCIETY OF CHEMISTRY

www.rsc.org/chemcomm

Journal Name RSCPublishing

COMMUNICATION

Cite this: DOI: 10.1039/x0xx00000x

Received 00th January 2012,
Accepted 00th January 2012

DOI: 10.1039/x0xx00000x

www.rsc.org/

Template-assisted *in situ* polymerization for blue organic light-emitting nanotubes

Li-Chi Lee [a], Han-Han[a], Yu-Tang Tsai[b], Gang-Lun Fan[a], Hsiang-Fang Liu[a], Chung-Chih Wu*[b], Jing-Jong Shyue[c], Shih-Sheng Sun[d], Chien-Liang Liu[a], Pi-Tai Chou[a] and Ken-Tsung Wong*[a]

A functional monomer was thermally polymerized inside the anodized aluminum oxide (AAO) channel into nanotubes, which were isolated and characterized to be semiconductive and blue fluorescent, and were utilized as a nano-container of Fe_3O_4 nanoparticles to form magnetic nanocomposite.

Recent advances in the interdisciplinary study of polymers with nanostructures have transformed fundamental researches into practical applications. Particularly, one-dimensional (1-D) conjugated polymeric nanomaterials, with their high aspect ratios, often induce photonic and electronic anisotropy that may be useful for realizing polarized emission and high charge mobility. As such, 1-D semiconductive polymers have been extensively studied for optoelectronic devices such as field effect transistors,[1] organic solar cells,[2] and organic light-emitting diodes (OLEDs).[3] A variety of synthetic strategies have been developed for preparing organic 1-D nanostructures, including self-assembly,[4] electrospinning,[5] nanolithography,[6] and physical vapor deposition.[7] In addition, porous anodized aluminum oxide (AAO) membraneswere adopted as the template to guide the growth of 1-D nanomaterials.[8] Using the templated wetting technique, AAO membranes can be utilized as nanomolds for forming small-molecule or polymer nanowires[9] or nanotubes[10]. However, these linear organic nanostructures may have low tolerance of organic solvents. Alternatively, the nanotubes formed by *in situ* polymerization with AAO templates possess covalently linked networks, thus giving strong resistance against organic solvents. For example, AAO can serve as the nanoreactor for electrodeposition of electro-active monomers to yield highly conductive polymers, such as polypyrrole, polythiophene, and polyaniline.[11] Yet more AAO-templated *in situ* polymerization for nanomaterials, such as [4+4] photocycloaddition of monomer with anthracene group for nanorods,[12] metal-catalyzed polymerization of styrene for polystyrene nanofibrils,[13] and thermal cross-linking of triphenylamine derivatives for nanoarrays,[14] had been reported. One crucial advantage of AAO-templated *in situ* polymerization is that the designated function(s) can be implanted on the monomer, rendering the preparation of functional nanotubes feasible. In this work, we expand the scope of AAO-templated *in situ* polymerization to make blue fluorescent semiconductive nanotubes using a precursor featuring a hole-transport (HT) core and two polymerizable styryl pendants. The hollow nanotubes can be further filled with Fe_3O_4 nanoparticles to make light-emitting magnetic nanocomposites.

Scheme 1 depicts the chemical structure of the functional monomer (**VB-FNPD**), which had been previously used to give high solvent tolerance and high-hole-mobility HT films for organic light-emitting devices (OLEDs) through thermal polymerization.[15] In **VB-FNPD,** the diarylamino groups attached to a rigid and planar fluorene core gives the monomer efficient blue fluorescence. In addition, the polymerizable styryl groups were attached to the HT-active core via an inert sp^3-hybridized carbon bridge to preserve the functionalities of mononer cores after thermal polymerization. The polymeric nanotubes were achieved by combining the template wetting and *in situ* thermal polymerization (Scheme S1, Electronic supplementary information ESI), which were then dispersed in ethanol for further characterization.

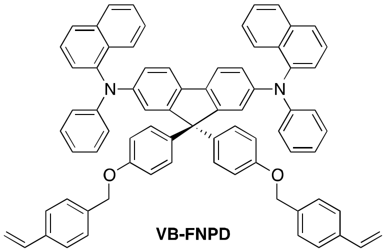

Scheme 1 The structure of **VB-FNPD**.

The morphologies of the thermally cross-linked **poly-**VB-FNPD nanotubes were characterized by SEM and TEM. The SEM images (Fig. 1a) of the sonication-dispersed nanotubes shows the average outer diameter of ~200 nm, corresponding nicely to the inner diameter of the AAO template channels. The lengths of nanotubes are ranging from several to tens of micrometers. The variations on lengths could be attributed to the ultrasonication and/or centrifugation-induced cracking of defected nanotubes, perhaps associated with incomplete coverage of the monomer solution over the AAO channels, the structural defects (branching), and the length variations of the AAO channels. The SEM image also indicates that exterior surfaces of nanotubes appear smooth and uniform. Meanwhile, the TEM image (Fig. 1b, also Fig. S1 in ESI) clearly reveals a pair of internal surfaces inside external surfaces, confirming the tubular nature of formed nanostructures and implying the potential for further modification. The TEM images also reveal the wall thickness to be about 25-50 nm, depending on the section location on the tube (e.g., near the tube end or center etc.) and AAO template properties.

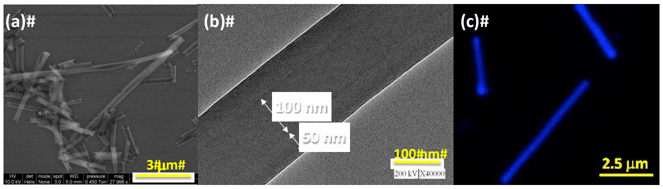

Fig. 1 Representative (a) SEM, (b) TEM, and (c) CLSM images of poly-**VB-FNPD** nanotubes.

The electronic absorption and photoluminescence (PL) spectra of nanotubes casted on a quartz slide show limited changes as compared to those of the monomer and thermally polymerized poly-**VB-FNPD** thin films (Fig. S2 in ESI). The PL quantum yields of poly-**VB-FNPD** nanotubes are 0.12 and 0.05 in EtOH and film, respectively, which are comparable to those of monomer (0.15 in EtOH, 0.07 in film). These results reveal the effectiveness of the molecular design strategy by introducing the polymerizable styryl groups onto the sp^3-hybridized carbon bridge to preserve the photophysical properties of the active chromophore core after the polymerization. The luminescence of the individual poly-**VB-FNPD** nanotube was probed by confocal laser scanning microscopy (CLSM) (Fig. 1c). As shown, the well-dispersed nanotubes were clearly identified for their clear contours and strong blue fluorescence.

For probing the mechanical behavior (stiff or flexible) of the poly-**VB-FNPD** nanotubes, we used a homemade nano-manipulator which combines a scanning probe microscope (SPM) with an inverted optical microscope (OM). The nanotube sample (in EtOH) was drop-casted onto a microscope slide (18 x18 mm). Then, the nanotubes were imaged by OM with an objector (100X), and manipulated by the SPM tip (radius 50 nm). As shown in the supporting video (see ESI), one of the casted nanotubes was initially bent. As the SPM tip landed to physically contact the sample, by controlling the PZT stage, the initially bent nanotube can be deformed by the SPM tip into a linear one, showing the flexibility of poly-**VB-FNPD** nanotubes.

The monomer **VB-FNPD** derived from the well-known HT material α-NPD should inherit the HT behavior of α-NPD. Therefore, the poly-**VB-FNPD** nanotube is expected to possess reasonable electrical conductivity. To probe the electronic behavior, the nano device (inset of Fig. 2) was fabricated by using focused-ion-beam (FIB) to make Pt contact to the nanotube between two ITO electrodes (Scheme S2 in ESI). The representative I-V curve shown in Fig. 2 reveals a quasi-linear characteristic for the bias voltage from -5 to 5 V. The extracted device resistance $R_{VB\text{-}FNPD}$ is ca. 5.0×10^{11} Ω. With the measured nanotube length L ~2.2 µm, mean outer diameter D ~200 nm, and wall thickness W~25-50 nm, the calculated nanotube resistivity $\rho = \pi R[D^2-(D-2W)^2]/4L \sim 1.8\text{-}3.1 \times 10^5$ Ω·cm and the conductivity $\sigma \sim 3.2\text{-}5.6 \times 10^{-6}$ S cm^{-1}, which is of similar magnitude to other reported polymer nanowires.[16] The other nano devices empolying naotubes with various lengths performed comparable conductivities (see Fig. S3), which are two order higher than that of a monomer film (Scheme S3 and Fig. S4).

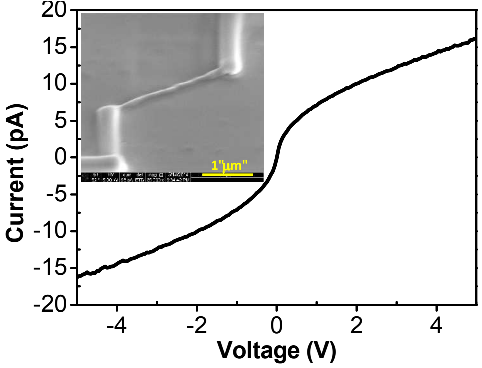

Fig. 2 Current-voltage (I-V) characteristics of the poly-**VB-FNPD** nanotube. The inset shows the SEM image of nano device fabricated by focus ion beam.

The protocol combining template-wetting and *in situ* thermal polymerization followed by the removal of template and sonicated dispersion renders possible not only the preparation of individual 1-D nanotubes, but also the ordered nanotube arrays with the support of transparent and flexible polystyrene substrates.[17] Before being subjected to de-template in aqueous KOH, the nanotube-implanted AAO membrane was pressed on a pre-heated (230 °C) melt polystyrene (PS) (Scheme S4 in ESI). After cooling to room temperature, the PS-supported AAO membrane was immersed into a 1 M KOH aqueous solution under sonication to remove the template. The SEM images (Fig. 3) clearly demonstrate that the poly-**VB-FNPD** nanotubes were successfully aligned, forming densely packed nanoarrays on top of the polystyrene. The nanoarray should approximately replicate the dimensions of the AAO channels with the estimated density of about 10^9 tubes per square centimeter and a mean height of about 50 µm. Since the nanotube is semiconductive and fluorescent, such nanoarrays may find potential applications in waveguides or microelectronics, for which the size and density of nanotubes can be customized by tailoring the AAO template.

Employing their hollow nature and the post wetting strategy, our organic light-emitting nanotubes (OLETs) can be utilized as nanocontainers to prepare nanocomposites with intriguing dual functions. Before removal of the template, the nanotube-implanted AAO membrane was impregnated with magnetic Fe_3O_4 nanoparticles (Fe_3O_4NP) (oleylamine/oleic acid capped, 12±1 nm, in ethanol), facilitated by an external magnetic field

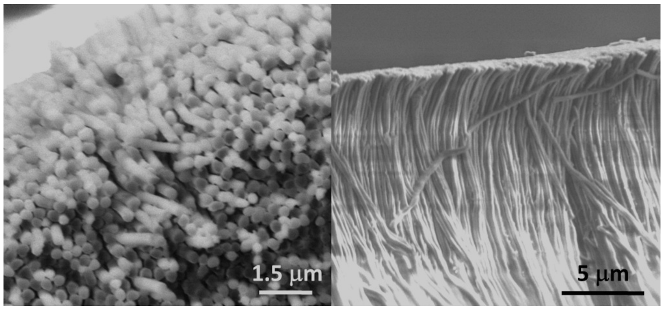

Fig. 3 SEM images of the array of poly-**VB-FNPD** nanotubes.

(Scheme S5 in ESI). The TEM image (Fig. 4e also Fig. S4 in ESI) clearly reveals the Fe$_3$O$_4$ nanoparticles introduced into and aggregating inside the nanotubes that were removed from the template. The bifunctional behavior of the Fe$_3$O$_4$NP/OLET nanocomposites is clearly demonstrated in Fig. 4a-4d. The aqueous solution of the dispersed magnetic nanocomposites (Fig. 4a) exhibited a strong blue emission under 365-nm UV light excitation (Fig. 4b). In the presence of a magnet (Fig. 4c), the nanocomposites were driven/located near the vial wall so that under UV excitation emission was observed only near the bottle rim. Such dual emission and positioning capabilities of the magnetic blue fluorescent OLETs may find some intriguing applications, e.g. bio-applications.[18]

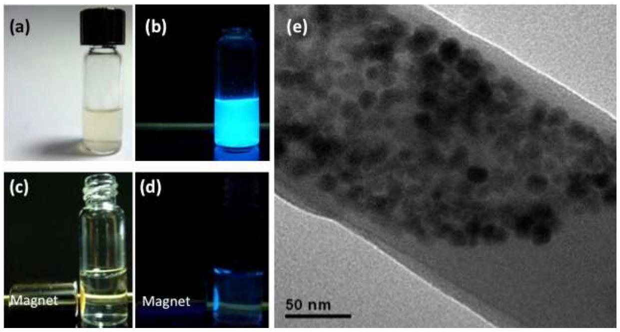

Fig. 4 (a) The Fe$_3$O$_4$/OLET nanocomposites dispersed in DI water. (b) The corresponding blue emission excited by 365-nm UV lamp. (c) The nanocomposites attracted to one side of the vial by a magnet and (d) excited by UV. (e) The TEM image of Fe$_3$O$_4$/OLET nanocomposites.

In summary, a functional monomer **VB-FNPD** derived from the well-known HT material α-NPD was utilized to make organic light-emitting poly-**VB-FNPD** nanotubes by virture of AAO-assisted template-wetting and *in situ* thermal polymerization. The new poly-**VB-FNPD** nanotubes were characterized with SEM, TEM, and CLSM, showing their hollow nature and intense blue fluorescence. Furthermore, the nanotubes exhibit mechanical flexibility and semi-conductivity as characterized by a nano-manipulator and a nano device fabricated by FIB, respectively. The nanotubes can be filled with Fe$_3$O$_4$ nanoparticles to prepare magnetic light-emitting nanotubes, giving new nanocomposites a positioning capability with magnetic forces. The isolation of polymerizable styryl groups from the fluorescence- and HT-active chromorphore core is the key feature for the nanotubes to preserve the optical properties of the monomer. Our established method shall allow one to make nanotubes with desired functions by tailoring the designated monomer in advance.

Notes and references

[a] *Department of Chemistry, National Taiwan University, Taipei 10617, Taiwan, E-mail: kenwong@ntu.edu.tw*
[b] *Department of Electrical Engineering, Graduate Institute of Electro-optical Engineering and Graduate Institute of Electronics Engineering, National Taiwan University, Taipei, 10617, Taiwan, E-mail: wucc@ntu.edu.tw*
[c] *Research Center for Applied Sciences, Acamedia Sinica 128 Academia Road, Nankang, Taipei 115, Taiwan*
[d] *Institute of Chemistry, Acamedia Sinica 128 Academia Road, Nankang, Taipei 115, Taiwan.*

† Electronic Supplementary Information (ESI) available: The UV-Vis absorption and photoluminescence spectra, the procedures for preparing the individual nanotubes, the nanotube arrays, the Fe$_3$O$_4$NP/blue-OLET nanocomposites, and the devices for electronic properties as well as the video for mechanical behavior. Please see DOI: 10.1039/b000000x

1 H. Sirringhaus, P. J. Brown, R. H. Friend, M. M. Nielsen, K. Bechgaard, B. M. W. Langeveld-Voss, A. J. H. Spiering, R. A. J. Janssen, E. W. Meijer, P. Herwig and D. M. de Leeuw, *Nature*, 1999, **401**, 685.
2 C.-Y. Chang, C.-E. Wu, S.-Y. Chen, C. Cui, Y.-J. Cheng, C.-S. Hsu, Y.-L. Wang and Y.-F Li, *Angew. Chem. Int. Ed.*, 2011, **50**, 9386.
3 (a) B. O'Connor, K. H. An, Y. Zhao, K. P. Pipe and M. Shtein, *Adv. Mater.*, 2007, **19**, 3897; (b) Q. Niu, Y. Zhou, L. Wang, J. Peng, J. Wang, J. Pei and Y. Cao. *Adv. Mater.*, 2008, **20**, 964; (c) V. Vohra, U. Giovanella, R. Tubino, H. Murata and C. Botta, *ACS Nano*, **5**, 5572.
4 C. Giansante, G. Raffy, C. Schäfer, H. Rahma, M.-T. Kao, A. G. L. Olive and A. D. Guerzo, *J. Am. Chem. Soc.*, 2011, **133**, 316.
5 H. Yang, C. R. Lightner and L. Dong, *ACS Nano*, 2012, **6**, 622.
6 A. Del Campo and E. Arzt, *Chem. Rev.*, 2008, **108**, 911.
7 Y. S. Zhao, H. B. Fu, F. Q. Hu, A. D. Peng, W. S. Yang and J. N. Yao, *Adv. Mater.* 2008, **20**, 79.
8 (a) S. J. Hurst, E. K. Payne, L. Qin and C. A. Mirkin, *Angew. Chem. Int. Ed.*, 2006, **45**, 2672; (b) M. R. Jones, K. D. Osberg, R. J. Macfarlane, M. R. Langille and C. A. Mirkin, *Chem. Rev.*, 2011, **111**, 3736; (c) Y. Liu, J. Goebl and Y. Yin, *Chem. Soc. Rev.*, 2013, **42**, 2610; (d) R. O. Al-Kaysi, T. H. Ghaddar and G. Guirado, *J. Nanomater.,* 2009, 436375; (e) J. Joo, K. T. Park, B. H. Kim, M. S. Kim, S. Y. Lee, C. K. Jeong, J. K. Lee, D. H. Park, W. K. Yi, S. H. Lee and K. S. Ryu *Synth. Met.,* 2003, **235-236**, 7; (f) R. K. Zheng, H. L. W. Chan and C. L. Choy, *Nanotechnology*, 2005, **16**, 1928.
9 (a) D. O'Carroll, I. Lieberwirth and G. Redmond, *Small*, 2007, **3**, 1178. (b) L. Qu and G. Shi. *Chem. Commun.,* 2004, 2800.
10 (a) M. Steinhart, J. H. Wendorff, A. Greiner, R. B. Wehrspohn, K. Nielsh, J. Schilling, J. Choi and U. Gösele, *Science*, 2002, **296**, 1997; (b) M. Steinhart, R. B. Wehrspohn, U. G and J. H. Wendorff, *Angew. Chem. Int. Ed.*, 2004, **43**, 1334; (c) S. Schlitt, A. Greiner and J. H. Wendorff *Macromolecules*, 2008, **41**, 3228.
11 C. R. Martin, *Science*, 1994, **266**, 1961.
12 R. O. Al-Kaysi, R. J. Dillon, J. M. Kaiser, L. J. Mueller, G. Guirado and C. J. Bardeen, *Macromolecules*, 2007, **40**, 9040.
13 K. Y. Choi, J. J. Han, B. He and S. B. Lee, *J. Am. Chem. Soc.*, 2008, **130**, 3920.
14 (a) N. Haberkorn, J. S. Gutmann and P. Theato, *ACS Nano*, 2009, **3**, 1415; (b) N. Haberkorn, S. A. L. Weber, R. Berger and P. Theato, *ACS Appl. Mater. Interfaces*, 2010, **2**, 1573.
15 C.-Y. Lin, Y.-C. Lin, W.-Y. Hung, K.-T. Wong, R. C. Kwong, S. C. Xia, Y.-H. Chen and C.-I. Wu, *J. Mater. Chem*., 2009, **19**, 3618.
16 G. A. O'Brien, A.J. Quinn, D. A. Tanner and G. Redmond, *Adv. Mater.* 2006, **18**, 2379.
17 H. Watanabe and T. Kunitake, *Chem. Mater.*, 2008, **20**, 4998.
18 (a) S. J. Son, J. Reichel, B. He, M. Schuchman and S. B. Lee, *J. Am. Chem. Soc.,* 2005, **127**, 7316; (b) V. Kumar, G. Nath, R.. K. Kotnala, P. S. Saxena and A. Srivastava, *RSC Adv.,* 2013, **3**, 14634.